Bias-Stress-Induced Charge Trapping at Polymer Chain Ends of Polymer Gate-Dielectrics in Organic Transistors

*Hyun Ho Choi, Wi Hyoung Lee, and Kilwon Cho**

Herein is demonstrated that the polymer chain ends of polymer gate-dielectrics (PGDs) in organic field-effect transistors (OFETs) can trap charges; the bias-stress stability is reduced without changes in the mobilities of the transistor devices as well as the morphologies of the organic semiconductors. The bias-stress stabilities of OFETs using PGD with various molecular weights (MWs) are investigated. Under bias stress in ambient air, the drain current decay and the threshold voltage shift are found to increase as the MW of the PGD decreases (MW effect). This MW effect is caused by the variation in the density of polymer chain ends in the PGDs with MW: the free volumes at the polymer chain ends act as charge-trap sites, resulting in drain current decay during bias stress. The free volumes at polymer chain ends are sufficiently large to allow the residence of water molecules, the presence of which significantly increases the density of charge-trap sites. In contrast, polymer chain ends without trapped water molecules do not allow charge trapping and so bias-stress stability is independent of the MW of the PGD. It is also found that the hydrophilicity/hydrophobicity of the chain ends of the PGD can affect bias-stress stability; carboxyl-terminated polystyrene exhibits a much higher trap density and lower bias-stress stability than hydrogen-terminated polystyrene when these devices are exposed to humid nitrogen.

1. Introduction

Charge trapping in semiconductors and gate-dielectrics determines the electrical properties of organic field-effect transistors (OFETs), including, most importantly, the threshold voltage (V_{th}) but also the FET mobility, the on-off current ratio, and hysteresis.[1–4] Remarkable advances in the performance of OFETs have been accomplished through increases in FET mobility.[5–9] However, the long-term operational reliability of OFETs is still inferior to that of silicon-based transistors and this inferiority is a major impediment to their commercialization.[10–13] When an OFET is driven with a continuous gate bias, i.e., under bias stress, the V_{th} usually shifts over time and this change corresponds to decay in the source-drain current (I_D). The commonly accepted mechanism of I_D decay under bias stress is the formation of carrier traps (trap formation). However, the actual locations of charge trap sites and the trapping mechanism are poorly understood.

Polymer gate-dielectrics (PGDs) are essential to the production of mechanically-flexible OFETs,[14–18] but can contain more charge trap sites than organic semiconductors (OSCs). In case of OFETs with PGDs, recent reports have demonstrated that most of the trapped charges that are the main cause of I_D decay under bias stress are located in the gate-dielectric and not in the semiconductor.[19,20] In those studies, the surface potential after bias stress is identical both with and without semiconductor, which indicates that the charges are not trapped in the semiconductor but mainly in the gate-dielectric. A clear understanding of the actual locations of trap sites in PGDs is crucial to the development of bias-stress stable OFETs.

Polymer chain-ends are closely related to the physical properties of a polymer. For example, variation in the chain-end density, which varies with the molecular weight (MW), has great effects on the glass transition temperature and viscoelasticity. These effects arise because polymer chain-ends have larger free volumes than chain-middles and thus have higher mobilities.[21] In an OFET, the mobility of PGD chain-ends affects the morphology of the OSC deposited on the PGD.[22] Moreover, a recent report has demonstrated that the presence of chain-ends on the surface of a PGD with low MW results in drastically lower FET mobilities when MW is below a critical value.[23] It was found that the surface energies of polymer chain-ends are different to those of polymer chain-middles, hence MW affects the grain size of the OSC and thus the mobility.

These above-mentioned reports suggest that PGD chain-ends influence the morphology of OSCs. However, no studies of the effects of the chain-end density of PGDs on the bias-stress stability of OFETs have been reported. Further, it has not previously been suggested that PGD chain-ends are the actual locations of the trap sites that reduce the bias-stress stability of OFETs. In this study, we demonstrated that PGD chain-ends can trap charges and then reduce bias-stress stability without changing FET mobilities as well as the OSC characteristics (morphology and crystallinity). This effect does not arise because PGD chain-ends have different surface energies from chain-middles, but

H. H. Choi, Dr. W. H. Lee, Prof. K. Cho
Department of Chemical Engineering
Center for Advanced Soft Electronics (CASE)
Pohang University of Science
and Technology (POSTECH)
Pohang 790-784, Korea
E-mail: kwcho@postech.ac.kr

DOI: 10.1002/adfm.201201084

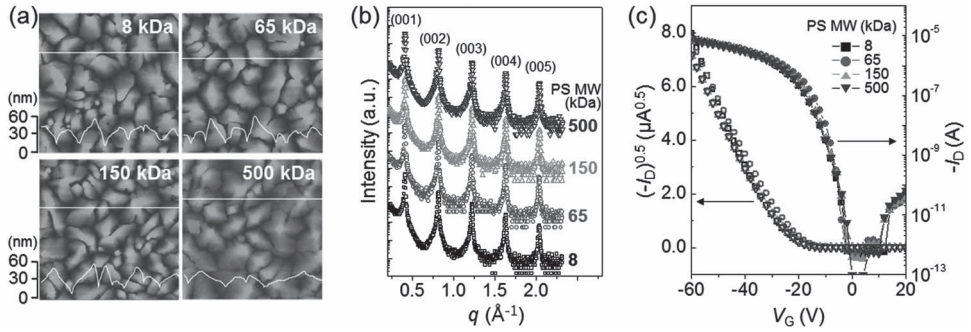

Figure 1. (a) AFM images (3 μm × 3 μm), and (b) X-ray diffraction patterns ($\theta/2\theta$ scan mode) of 50 nm thick pentacene films on PS gate-dielectrics with various MWs. (c) Transfer curves in the saturation regime ($V_D = -60$ V) for pentacene FETs using PS gate-dielectrics with various MWs.

because PGD chain-ends have much higher free volumes than chain-middles.

2. Results and Discussion

In this study, we varied the density of polymer chain-ends which are possible charge trap sites under bias stress by varying the MW of the polymer (polystyrene, PS). PS samples with MWs from 8 to 500 kDa and very narrow MW distributions (polydispersity index, PDI ≤ 1.05) were used as PGDs. The chain-ends of anionic polymerized PS have *sec*-butyl and hydrogen end groups. Previous reports have suggested that the surface energy of PS films decreases with MW only when MW < 8 kDa and is essentially independent of MW when MW ≥ 8 kDa.[22,23] The measured water contact angles of the PS films (~91°) were found to be consistently independent of MW in our study. Top-contact and bottom-gate transistor device architecture was used. To suppress the migration of charge carriers from the gate electrode and to increase the breakdown strength of the dielectric, a SiO_2 insulator was inserted between the 150 nm thick layer of PS and the gate (*n*-doped Si). The measured capacitance (C_i) of the PGD/SiO_2 was found to be independent of the PS MW (6.1 nF cm^{-2} at 30 kHz). A 50 nm thick layer of pentacene deposited on the PGD at room temperature was used as the OSC.

First, we examined the variations in morphology and crystallinity of OSCs deposited on the PGDs with various MWs. We obtained AFM images (**Figure 1**a) and X-ray diffraction patterns ($\theta/2\theta$ scan mode) (Figure 1b) of 50 nm thick pentacene films thermally deposited on the PS PGDs. The grain sizes, (00*l*) peak intensities, and the values of the full width of half maximum (FWHM) of the (00*l*) peaks for the various PS samples are almost same regardless of PS MW. Thus, the morphologies and crystalline ordering of the pentacene film are not significantly affected by variation of the PS MW in the range 8 to 500 kDa. Hence, we expect the electrical properties of the devices are not affected much by the PS MW. Transfer curves were determined for the devices with PS PGDs with different MWs (8, 65, 150 and 500 kDa) before bias stress (Figure 1c). The FET mobilities (μ) and threshold voltages (V_{th}) were extracted from the equation

$$I_D = \frac{W}{2L}\mu C_i (V_G - V_{th})^2 \quad (1)$$

where I_D is the source-drain current, W is the channel width, L is the channel length, and V_G is the gate voltage.[1] Calculated values of μ (0.7 cm^2 V^{-1}s^{-1}) and V_{th} (–27.5 V) for the devices with different PGD MW are very similar (**Table 1**).

However, the electrical characteristics are strongly dependent on the PS MW when bias stress is applied. The time dependence of I_D decay was measured at room temperature and 25% relative humidity (RH) under constant bias stress (V_G = –60 V, drain voltage V_D = –5 V) for 3 h (**Figure 2**a). The obtained results show that the decay in the values of the normalized I_D (= $I_D(t)/I_D(0)$, where t = time and $I_D(0)$ is I_D before bias stress) increases remarkably as the PS MW decreases (Figure 2a); after 3 h bias stress, the value of the normalized I_D is lower in the transistor device with 8 kDa PS (0.65) than in the device with 500 kDa PS (0.85). This difference, which we name the MW effect, suggests that charge traps in a deep state are formed in the PS gate-dielectric, and that the charge trap density increases as the PS MW decreases.

The bias stress in our experiment was applied in the linear region ($V_G \gg V_D$) and μ was constant during bias stress (Figure S1 of the Supporting Information). Under these this conditions, the I_D decay can be fitted with a stretched exponential function (solid line, Figure 2a):[12,24]

$$I_D(t) = I_0(0)\exp\left[-\left(\frac{t}{\tau}\right)^{\beta}\right] \quad (2)$$

where β is the dispersion parameter and τ is the characteristic time. If τ is small, I_D decay is fast. When plotted against the PS

Table 1. Field-effect mobilities (μ) and threshold voltages (V_{th}) of pentacene FETs using PS gate-dielectrics with various MWs before bias stress.

	Molecular weight of PS			
	8 kDa	65 kDa	150 kDa	500 kDa
μ [cm^2 V^{-1} s^{-1}]	0.71	0.70	0.77	0.70
V_{th} [V]	–28.4	–28.8	–26.3	–27.4

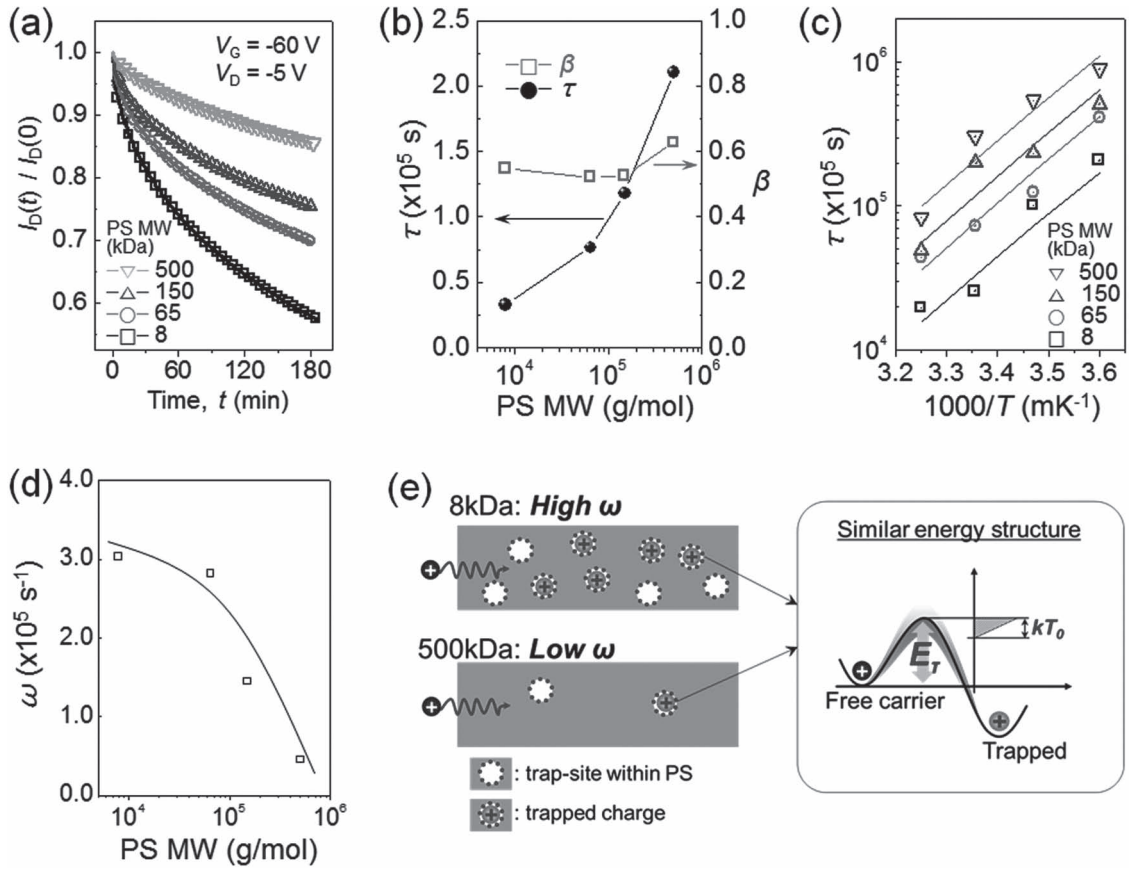

Figure 2. (a) Time-dependent I_D decay under constant bias-stress (V_G = −60 V, V_D = −5 V) in ambient air. Open circles: experimental results. Solid lines: the stretched exponential function $I_D(t) = I_D(0)\exp[-(t/\tau)^{\beta}]$ fitted to the experimental results. (b) Plots of τ and β as functions of the PS MW. (c) Arrhenius plot of τ as a function of 1000/T (temperature). Solid lines: linear fits of $\tau = \omega^{-1}\exp(E_\tau/kT)$ to the experimental results. (d) Plot of MW-dependent ω extracted from the y-intercepts of the linear fits in Figure 2c. (e) Schematic diagram showing the effects of MW on the bias-stress stability and charge trapping; the key contribution to MW-dependent bias-stress stability is that of ω, not E_τ or β.

MW, β does not change significantly but τ increases with MW (Figure 2b). Therefore, in our experiment, variation in τ is the key contribution to the MW effect.

The parameter τ has an Arrhenius-type temperature dependence.[12,24]

$$\tau = \omega^{-1}\exp(E_\tau/kT) \quad (3)$$

where ω is the frequency prefactor, E_τ is the mean activation energy of trapping, k is the Boltzmann constant and T is the absolute temperature. To further analyze τ, we measured τ for $278 \le T \le 308$ K; the Arrhenius plot is shown in Figure 2c. The slope and y-intercept of the linear fits correspond to E_τ and $-\ln(\omega)$, respectively. The resulting value of E_τ is independent of the PS MW, but ω decreases as MW increases (Figure 2d). This result indicates that the MW dependence of τ is due to the MW dependence of ω.

The contribution of ω to the MW effect is expressed schematically (Figure 2e). The stretched exponential function is derived from the diffusion theory of charges, in which the time-dependent diffusion coefficient of charges $D(t)$ is given by $D(t) = D_0(\omega t)^{-1/\beta}$, where D_0 is the diffusion coefficient at time 0.[25–27] The frequency prefactor ω is a trap attempt frequency that is proportional to the density of trap sites in which charge carriers are prone to be trapped under bias stress.[28] A high value of ω corresponds to a high density of trap sites. In our experiment, the increases in ω with decreases in the PS MW correspond to an increase in the number of charge trap sites within PS PGD as MW decreases; this increase causes the increase in the I_D decay.

In contrast, the energy structure of each trap site, which can be described in terms of E_τ and kT_0, is independent of the PS MW. E_τ is the mean barrier height for charge trapping, and kT_0 (= kT/β) is the barrier distribution (Figure 2e right).[24] E_τ and β are independent of the PS MW (Figure 2b,c), so the energy structure of the trap sites in PS is not affected by variation in the PS MW. It has been reported that the energy structures of trap sites (E_τ and β) are strongly affected by the chemical nature of semiconductors and gate-dielectric.[12,24,29] Therefore, we conclude that the trap sites contributing to the MW effect have the same energy structures regardless of PS MW due to the same chemical structure of them, and that the increase in their density for low MW PS results in the increased I_D decay under bias stress (**Table 2**).

Table 2. Summary of MW-dependent parameters for the stretched exponential function: dispersion parameter (β), characteristic time (τ), mean-activation energy for charge trapping (E_τ), and frequency prefactor (ω).

	Molecular weight of PS			
	8 kDa	65 kDa	150 kDa	500 kDa
β	0.55	0.52	0.53	0.63
τ [$\times 10^5$ s]	3.26	7.66	11.8	21.0
E_τ [eV]	0.59	0.61	0.61	0.59
ω [$\times 10^5$ s^{-1}]	3.03	2.82	1.45	0.45

We hypothesize that the higher trap density of a device with low-MW PS occurs because the density of PS chain-ends is higher in low-MW PS than in high-MW PS. Generally, there is more free volume at a chain-end of a polymer chain than in the middle of the chain.[30–32] Such empty spaces can serve as defect sites in PGDs, resulting in charge trapping. To test our hypothesis, we measured the bias-stress instabilities of OFETs fabricated using blends of PS with two different MWs (8 and 500 kDa) in various ratios (**Figure 3**a). An increase in the proportion of 8 kDa PS corresponds to an increase in the density of PS chain-ends in the PGD. The result shows that I_D decay increases with increases in the weight percentage of 8 kDa PS. As is consistent with the MW effect in Figure 2b, the fitted parameter τ decreases linearly with increases in the proportion of 8 kDa PS, whereas the β is independent of the proportion of 8 kDa PS (Figure 3b). It is obvious that the MW effect under bias stress is due to variation in the PS chain-end density, and that PS chain-ends trap charges in deep states thereby decreasing I_D during bias stress. This conclusion raises a new question: why do charge trap sites prefer to form at PS chain-ends rather than PS chain-middles?

To investigate the mechanism of charge trapping at polymer chain-ends, bias stress was applied in a vacuum to devices containing PS gate-dielectrics with various MWs. The time-dependent I_D decays of the devices under constant bias stress (V_G = –60 V, V_D = –5 V) were obtained (**Figure 4**a). Interestingly,

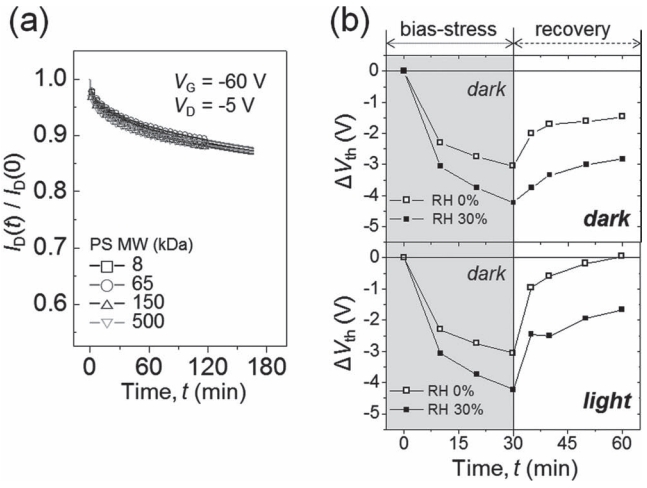

Figure 4. (a) Time-dependent I_D decay under constant bias-stress (V_G = –60 V, V_D = –5 V) in a vacuum. Open circles, experimental results; solid lines, fits to the experimental results with the stretched exponential function ($I_D(t) = I_D(0)\exp\{-(t/\tau)^\beta\}$). (b) Time-dependent ΔV_{th} of the device using 8 kDa PS gate-dielectric at RH = 0% (□) and 30% (■). Bias stress (V_G = –60 V, V_D = 0 V) was applied under dark conditions for 30 min, and then the recovery process ($V_G = V_D$ = 0 V) was performed in darkness (top) or under illumination (bottom).

all of the devices exhibited the same I_D decay regardless of the PS MW; these results differ greatly from those obtained in ambient air (Figure 2a). The disappearance of the PS MW effect in a vacuum indicates that the PS chain-ends do not contribute to the bias-stress instability in a vacuum. Thus, we can speculate that PS chain-ends preferentially adsorb certain molecules in air, and only certain molecule-adsorbed chain-ends form charge trap sites.

We found that the molecule that results in the MW effect is water. The presence of water molecules in a device has previously been shown to be critically responsible for bias-stress instability.[33–38] To investigate the role of water molecules in the MW effect, we conducted electrical measurements under bias stress and recovery under well-controlled relative humidity (RH) conditions in presence of nitrogen and water. Changes in the threshold voltage shift (ΔV_{th}) over time were measured in a device containing 8 kDa PS at RH = 0% and 30% (Figure 4b). Bias stress (V_G = –60 V, V_D = 0 V) was applied in darkness for 30 min, and then the recovery process ($V_G = V_D$ = 0 V) was performed in darkness (Figure 4b, top), or under illumination (Figure 4b, bottom) for 30 min. Under bias stress, the absolute value of the threshold voltage shift, $|\Delta V_{th}|$ was found to be greater at 30% RH than at 0% RH, which implies that this process is caused by water-assisted charge trapping. Considering the recovery process, the ΔV_{th} results show that there are two different charge detrapping mechanisms that are independent of RH: fast and slow. The fast charge detrapping occurs during the initial stages only when the device

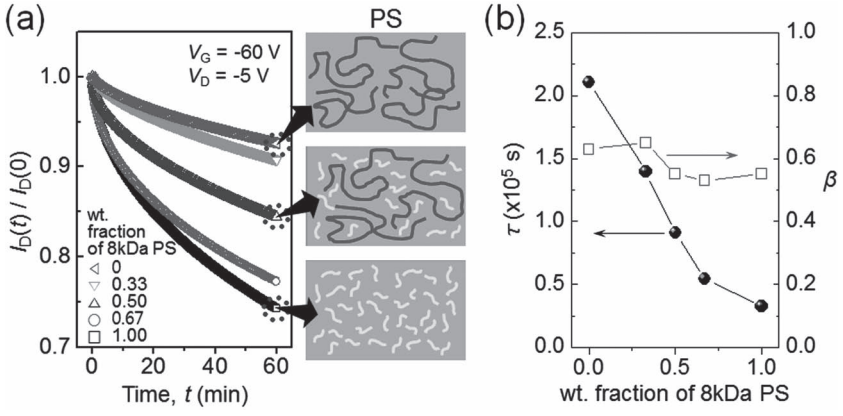

Figure 3. (a) Time-dependent I_D decay of pentacene FETs using PS gate-dielectrics with various weight fractions of 8 kDa PS in (8 kDa + 500 kDa) PS films under constant bias stress (V_G = –60 V, V_D = –5 V) in ambient air. (b) Plots of τ and β *vs* the weight fraction of 8 kDa PS.

is exposed to light. This light-induced removal of trapped charges is usually regarded as evidence for the photo-excitation of trapped charges, especially in OSCs.[39–41] The slow charge detrapping in the later stages always occurred regardless of photo-illumination, at a rate that was also independent of RH. We speculate that slow charge detrapping in the later stages is related to the presence of other trap sites within the PS gate-dielectric, and that these trap sites do not need water molecules to trap charges. One interesting point is that the difference between ΔV_{th} at RH = 30% and that at 0% after 30 min bias stress (1.3 V) remained almost the same, even after 30 min recovery both in dark and under illumination. This result implies that the water-assisted charge trap sites are located in the PS gate-dielectric. This difference is also consistent with the difference between the results in Figure 2a and 4a. Thus, the MW effect is strongly related to trapped charges associated with water molecules in PS. Even though 50 nm thick pentacene is deposited on the PS film, the pentacene layer does not prevent the diffusion of water molecules into PS because the capillary force of pentacene grain boundaries can attract water molecules.[38,42]

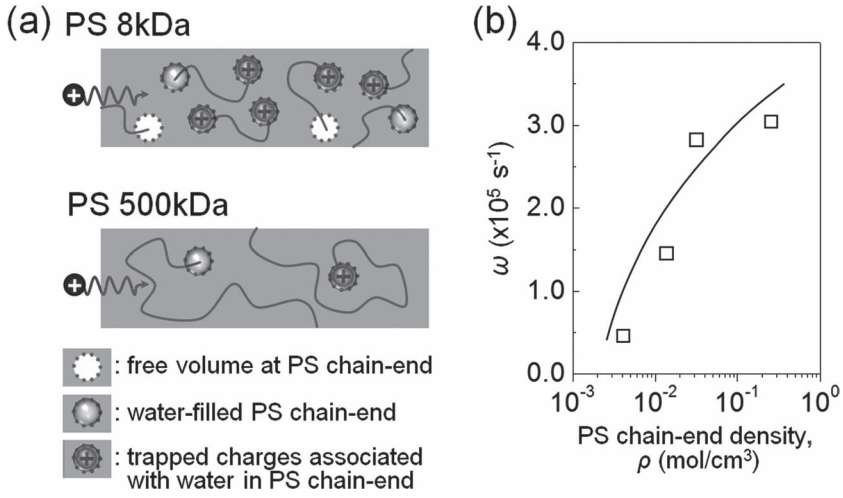

Figure 5. (a) Schematic diagrams showing a possible mechanism for the MW-dependent electrical instability (charge trapping) of PGDs. (b) Plot of ω *vs* PS chain-end density ρ.

We surmise that water molecules can diffuse into a PS gate-dielectric through the free volumes at the PS chain-ends. The difference between the surface energies of the PS chain-ends and chain-middles is not a driving force for water diffusion because the surface energies of PS chain-ends are slightly lower (23.0–30.5 mN m^{-1}) than those of the chain-middle (45.1 mN m^{-1}).[23,43] In general, the size of free volume at a PS chain-end is in the range of 35–180 $Å^3$, which is approximately 14 times larger than that at PS middle,[32,44] and is significantly larger than a water molecule (~10 $Å^3$). Thus, the diffused water molecules in PS quite probably reside in the free volumes of PS chain-ends. These water molecules confined in the free volumes at PS chain-ends are unable to form a crystalline structure; thus water might form a metastable liquid, i.e., supercooled water or glassy water.[45] This metastable water behaves electrically as a charge trap, which causes bias-stress instability.

Finally, we propose a mechanism (**Figure 5**a) for the MW-dependent bias-stress stability. Under bias stress, 1.3–1.8 MV cm^{-1} of electric field is applied to the PS. The electric field might allow polar water molecules to diffuse into PS chain-ends. PS chain-ends with water molecules can attract mobile holes, thereby inducing charge trapping. Water molecules incorporated into PS chain-end behave electrically as charge traps and decrease bias-stress stability. Therefore, in ambient air, the higher density of PS chain-ends for lower MW PS leads to an increase in the number of charge trap sites, resulting in an increase in the trap attempt frequency. We calculated the chain-end densities of PS samples with various MWs,[46] and plotted experimentally determined values of ω as a function of the PS chain-end density (Figure 5b). As expected, ω increases with chain-end density, which supports our proposed mechanism of chain-end-mediated charge trapping. The energy structure of metastable water molecules at PS chain-ends is not affected by the PS MW, and kT_0 and E_τ should be independent of the PS MW as shown in Figure 2b and c, respectively.

Our conclusion that PS chain-ends contribute to charge-trapping behavior implies that the hydrophilicity/hydrophobicity of PS chain-ends will affect the adsorption of water molecules and bias-stress stability. We measured the bias-stress stability of OFETs with H end-terminated PS (H-PS) and COOH end-terminated PS (COOH-PS) gate-dielectrics. The MWs of H-PS and COOH-PS are both 10 kDa. The density of PS chain-ends is much lower than that of PS chain-middles, so the surface energies of the PS chain-end have little effect on those of the PS film. Consequently, the measured water contact angles of H-PS and COOH-PS are similar (~91°). Hence, the AFM morphologies of 50 nm thick pentacene films on the H-PS and COOH-PS gate-dielectrics are similar (**Figure 6**a-I, 6b-I), as are the FET mobilities of the devices (Figure 6a-II, 6b-II). However, the trends in ΔV_{th} vs bias-stress time are significantly different. The applied gate bias during bias stress was −80 V for 1 h in dry N_2 or humid N_2 (30% RH) environments. The time dependent transfer curves of pentacene FETs with H-PS and COOH-PS were measured in dry N_2; $|\Delta V_{th}|$ was found to be slightly larger in the device with COOH-PS (Figure 6b-II) than in the device with H-PS (Figure 6a-II). This result implies that the COOH chain-ends without water molecules rather contribute to charge trap sites, but do not significantly degrade the bias-stress stability. The difference between the bias-stress instabilities of the devices with H-PS and COOH-PS increases when bias stress is applied in humid N_2 (30% RH) (Figure 6a-III, 6b-III). Thus, COOH-PS provides a much higher trap density than H-PS when the devices are exposed to water vapor. This difference arises because water molecules are attracted more strongly to the hydrophilic COOH end-groups than to the hydrophobic H end-group.

3. Conclusions

In this study, we investigated trap formation in the polymer gate-dielectrics of OFETs under bias stress. We found that

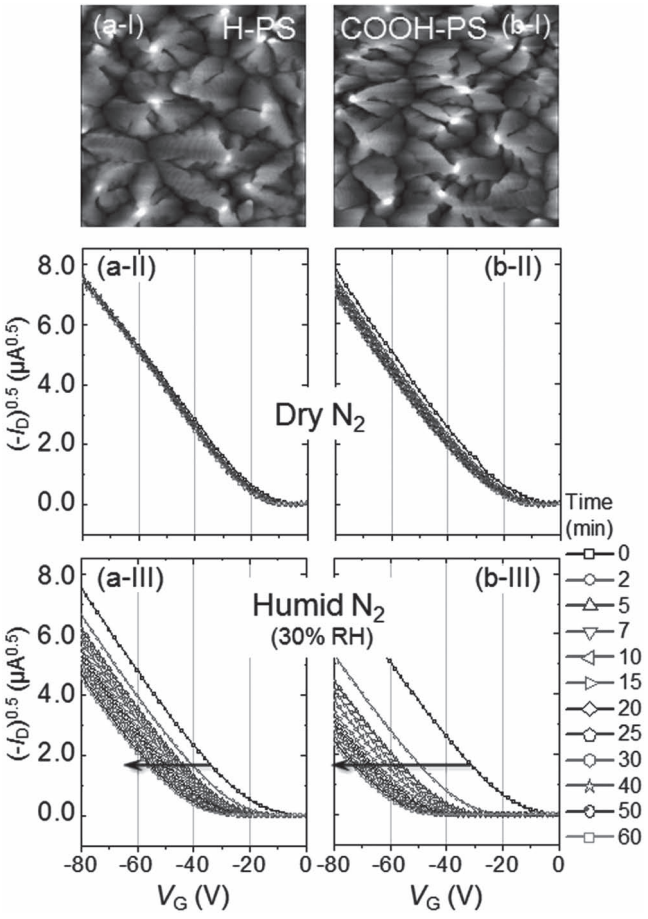

Figure 6. AFM morphologies of 50 nm thick pentacene on (a-I) H end-terminated PS (H-PS, MW = 10 kDa) and (b-I) COOH end-terminated PS (COOH-PS, MW = 10 kDa). The scan area is 3×3 μm^2. Time-dependent transfer curves of pentacene FETs with (a-II, a-III) H-PS and (b-II, b-III) COOH-PS under bias stress ($V_G = -80$ V) in (a-II, b-II) dry (100% N_2) and (a-III, b-III) humid environments (30% H_2O + 70% N_2).

variation in the MW of the PGD significantly influences the bias-stress stability of OFETs, but does not affect semiconductor morphology and FET mobility. We showed that the key contribution to the MW effect is the density of polymer chain-ends. Without water vapor, polymer chain-ends rarely function as charge trap sites, so variation in MW does not affect the bias stress stability. However, in the presence of water vapor, the chain-ends attract mobile holes, thereby inducing charge trapping. The mobile holes are attracted because the free volumes at polymer chain-ends are large enough to allow residence of water molecules, which reduces the energy barrier for charge trapping. The results and conclusions obtained in this study are vital to the design of PGDs for OFETs with enhanced bias-stress stability.

4. Experimental Section

PS ($8 \leq$ MW ≤ 500 kDa) with PDI ≤ 1.05 was purchased from Polymer Source Inc. The PS was recrystallized to remove impurities (such as salts). Pentacene was purchased from Aldrich. A highly doped *n*-Si wafer with a 300 nm thick thermally-grown SiO_2 layer was used as a substrate. In order to eliminate hydroxyl groups from the surface of SiO_2, the substrate was chemically treated with hexamethyldisilazane (HMDS, Aldrich) by baking (120 °C, 1 h) followed by spin-coating. Toluene solutions of PS with various MWs were spin-coated onto the HMDS-treated SiO_2/Si substrate. Well-defined 150 nm thick layers of PS were spin-coated by changing the concentration (wt%) of the solution and spin-speed (rpm) for each PS solution, and following the empirical equation, thickness (nm) = $241.2 \cdot (\text{wt\%}) \cdot (\text{rpm})^{-0.5} \cdot (\text{MW})^{0.25}$.[47] The thickness of each PS film was determined with an ellipsometer. The PS films were dried in a vacuum for >2 days to remove residual solvent. Next, 50 nm thick pentacene films were thermally evaporated onto PS under vacuum (~10^{-6} Torr). 50 nm thick Au layers were used as source-drain electrodes; the channel width (W) and length (L) were 1000 and 100 μm respectively.

The morphologies of the 50 nm thick pentacene films were analyzed with a Veeco NanoScope IIIa atomic force microscope; their molecular ordering was analyzed by using X-ray diffraction ($\theta/2\theta$ mode) at the 10C1 beamline of Pohang Acceleration Laboratory. All OFETs were characterized with a Keithley 2636A SourceMeter. The bias-stress experiments were conducted under various conditions such as ambient air, vacuum, dry nitrogen, and well-controlled water/nitrogen environments. The temperature dependence of τ (Figure 2b) was determined by conducting bias-stress experiments at various substrate temperatures. To avoid the thermal motion of polymer chains above surface glass transition temperature, the narrow temperature interval (5, 15, 25, and 35 °C) was chosen. To measure changes in the electrical properties under light illumination, a white beam (26 mW mm^{-2}) was shone onto the devices during the recovery process. To calculate chain-end densities, we followed the method of a previous report.[46]

Supporting Information

Supporting Information is available from the Wiley Online Library or from the author.

Acknowledgements

This work was supported by a grant (Code No. 2011-0031628) from the Center for Advanced Soft Electronics under the Global Frontier Research Program of the Ministry of Education, Science and Technology, Korea.

Received: April 18, 2012
Published online: July 9, 2012

[1] G. Horowitz, *Adv. Mater.* **1998**, *10*, 365.
[2] Y. D. Park, J. A. Lim, H. S. Lee, K. Cho, *Mater. Today* **2007**, *10*, 46.
[3] C. Reese, M. Roberts, M.-m. Ling, Z. Bao, *Mater. Today* **2004**, *7*, 20.
[4] D. H. Kim, H. S. Lee, H. Yang, L. Yang, K. Cho, *Adv. Funct. Mater.* **2008**, *18*, 1363.
[5] Q. X. Tang, H. X. Li, M. He, W. P. Hu, C. M. Liu, K. Q. Chen, C. Wang, Y. Q. Liu, D. B. Zhu, *Adv. Mater.* **2006**, *18*, 65.
[6] Y. Yamashita, *Sci. Technol. Adv. Mater.* **2009**, *10*, 0234313.
[7] S. Dasgupta, R. Kruk, N. Mechau, H. Hahn, *ACS Nano* **2011**, *5*, 9628.
[8] J. A. Lim, F. Liu, S. Ferdous, M. Muthukumar, A. L. Briseno, *Mater. Today* **2010**, *13*, 14.
[9] K. Nakayama, Y. Hirose, J. Soeda, M. Yoshizumi, T. Uemura, M. Uno, W. Li, M. J. Kang, M. Yamagishi, Y. Okada, E. Miyazaki, Y. Nakazawa, A. Nakao, K. Takimiya, J. Takeya, *Adv. Mater.* **2011**, *23*, 1626.

[10] W. H. Lee, J. H. Cho, K. Cho, *J. Mater. Chem.* **2010**, *20*, 2549.
[11] H. Sirringhaus, *Adv. Mater.* **2009**, *21*, 3859.
[12] D. M. de Leeuw, S. G. J. Mathijssen, M. Colle, H. Gomes, E. C. P. Smits, B. de Boer, I. McCulloch, P. A. Bobbert, *Adv. Mater.* **2007**, *19*, 2785.
[13] S. J. Zilker, C. Detcheverry, E. Cantatore, D. M. de Leeuw, *Appl. Phys. Lett.* **2001**, *79*, 1124.
[14] W. H. Lee, D. Kwak, J. E. Anthony, H. S. Lee, H. H. Choi, D. H. Kim, S. G. Lee, K. Cho, *Adv. Funct. Mater.* **2012**, *22*, 267.
[15] A. Facchetti, M. H. Yoon, T. J. Marks, *Adv. Mater.* **2005**, *17*, 1705.
[16] M. Halik, H. Klauk, U. Zschieschang, G. Schmid, W. Radlik, W. Weber, *Adv. Mater.* **2002**, *14*, 1717.
[17] X. Cheng, M. Caironi, Y.-Y. Noh, J. Wang, C. Newman, H. Yan, A. Facchetti, H. Sirringhaus, *Chem. Mater.* **2010**, *22*, 1559.
[18] M. J. Panzer, C. D. Frisbie, *J. Am. Chem. Soc.* **2007**, *129*, 6599.
[19] S. G. J. Mathijssen, M.-J. Spijkman, A.-M. Andringa, P. A. van Hal, I. McCulloch, M. Kemerink, R. A. J. Janssen, D. M. de Leeuw, *Adv. Mater.* **2010**, *22*, 5105.
[20] R. J. Young, P. A. Lovell, *Introduction to Polymers*, CRC Press, Boca Raton **2011**.
[21] C. Kim, A. Facchetti, T. J. Marks, *Science* **2007**, *318*, 76.
[22] Y. Q. Liu, X. N. Sun, C. A. Di, Y. G. Wen, Y. L. Guo, L. Zhang, Y. Zhao, G. Yu, *Adv. Mater.* **2011**, *23*, 1009.
[23] S. Wu, *Polymer Interface and Adhesion*, M. Dekker, New York **1982**.
[24] K. Tsukagoshi, T. Miyadera, S. D. Wang, T. Minari, Y. Aoyagi, *Appl. Phys. Lett.* **2008**, *93*, 033304.
[25] H. Scher, E. W. Montroll, *Phys. Rev. B* **1975**, *12*, 2455.
[26] M. Grünewald, B. Pohlmann, B. Movaghar, D. Würtz, *Philos. Mag. B* **1984**, *49*, 341.
[27] W. B. Jackson, J. M. Marshall, M. D. Moyer, *Phys. Rev. B* **1989**, *39*, 1164.
[28] J. Kakalios, R. A. Street, W. B. Jackson, *Phys. Rev. Lett.* **1987**, *59*, 1037.
[29] T. N. Ng, J. A. Marohn, M. L. Chabinyc, *J. Appl. Phys.* **2006**, *100*, 084505.
[30] Y. Miwa, T. Tanase, K. Yamamoto, M. Sakaguchi, M. Sakai, S. Shimada, *Macromolecules* **2003**, *36*, 3235.
[31] O. K. C. Tsui, H. F. Zhang, *Macromolecules* **2001**, *34*, 9139.
[32] W. C. Yu, C. S. P. Sung, R. E. Robertson, *Macromolecules* **1988**, *21*, 355.
[33] T. Jung, A. Dodabalapur, R. Wenz, S. Mohapatra, *Appl. Phys. Lett.* **2005**, *87*, 182109.
[34] M. L. Chabinyc, F. Endicott, B. D. Vogt, D. M. DeLongchamp, E. K. Lin, Y. L. Wu, P. Liu, B. S. Ong, *Appl. Phys. Lett.* **2006**, *88*, 113514.
[35] S. G. J. Mathijssen, M. Kemerink, A. Sharma, M. Coelle, P. A. Bobbert, R. A. J. Janssen, D. M. de Leeuw, *Adv. Mater.* **2008**, *20*, 975.
[36] C. Goldmann, D. J. Gundlach, B. Batlogg, *Appl. Phys. Lett.* **2006**, *88*, 063501.
[37] K. P. Pernstich, D. Oberhoff, C. Goldmann, B. Batlogg, *Appl. Phys. Lett.* **2006**, *89*, 213509.
[38] D. Li, E.-J. Borkent, R. Nortrup, H. Moon, H. Katz, Z. Bao, *Appl. Phys. Lett.* **2005**, *86*, 042105.
[39] A. Salleo, R. A. Street, *Phys. Rev. B* **2004**, *70*, 235324.
[40] R. A. Street, A. Salleo, M. L. Chabinyc, *Phys. Rev. B* **2003**, *68*, 085316.
[41] A. Salleo, F. Endicott, R. A. Street, *Appl. Phys. Lett.* **2005**, *86*, 263505.
[42] T. Someya, H. E. Katz, A. Gelperin, A. J. Lovinger, A. Dodabalapur, *Appl. Phys. Lett.* **2002**, *81*, 3079.
[43] J. F. Elman, B. D. Johs, T. E. Long, J. T. Koberstein, *Macromolecules* **1994**, *27*, 5341.
[44] J. Liu, Q. Deng, Y. C. Jean, *Macromolecules* **1993**, *26*, 7149.
[45] H. L. Gomes, P. Stallinga, M. Colle, D. M. de Leeuw, F. Biscarini, *Appl. Phys. Lett.* **2006**, *88*, 082101.
[46] K. Tanaka, D. Kawaguchi, Y. Yokoe, T. Kajiyama, A. Takahara, S. Tasaki, *Polymer* **2003**, *44*, 4171.
[47] D. Schubert, *Polym. Bull.* **1997**, *38*, 177.